

# System Noise Temperature Investigation of the DSN S-Band Polarization Diverse Systems for the Galileo S-Band Contingency Mission

J. E. Fernandez and D. L. Trowbridge  
Communications Ground Systems Section

*This article describes measurements made at all three Deep Space Network 70-m S-band polarization diverse (SPD) systems to determine and eliminate the cause of the 1-K elevation in follow-up noise temperature in the listen-only mode of the SPD systems at DSS 43 and DSS 63. The system noise temperatures obtained after finding and correcting the cause of the elevated follow-up noise temperature are also reported.*

## I. Introduction

In response to the Galileo spacecraft's X-band (8.45 GHz) antenna deployment failure, an emergency effort to optimize S-band (2.3 GHz) downlink performance was conducted. As part of this effort, termed the Galileo S-band Contingency Mission, the three 70-m DSN S-band polarization diverse (SPD) systems in the listen-only mode (see Fig. 1) have been carefully evaluated. Results of this initial evaluation were that both DSS 43 and DSS 63 at the Canberra and Madrid Deep Space Communications Complexes, respectively, exhibited elevated follow-up noise temperature contributions—defined as the contribution to system operating noise temperature of all components following the first low-noise amplifier (LNA)—of 1.25 K in comparison with the predicted values of 0.35 K. The system noise temperature predictions for these systems are shown in Tables 1 and 2. During the course of the evaluation, DSS-43 personnel determined the cause of this elevated follow-up noise temperature contribution in their 70-m SPD system to be due to a nonstandard configuration. This problem was corrected, and the antenna subsequently performed within predicted performance limits.

The reason for the elevated follow-up noise temperature at DSS 63, also determined during the course of this work, was a higher than normal attenuation level in the system path behind the maser LNA. Once this attenuation was reduced by about 4 dB, the measured follow-up noise temperature at DSS 63 of 0.4 K agreed very closely with the predicted value of 0.35 K. Also documented during the course of the investigation were high and dissimilar noise figures of the S-band Block IV receivers at DSS 14, as well as differences in gain of the right-hand circular polarization (RCP) and left-hand circular polarization (LCP) channels of the very long baseline interferometry (VLBI) downconverter at DSS 63.

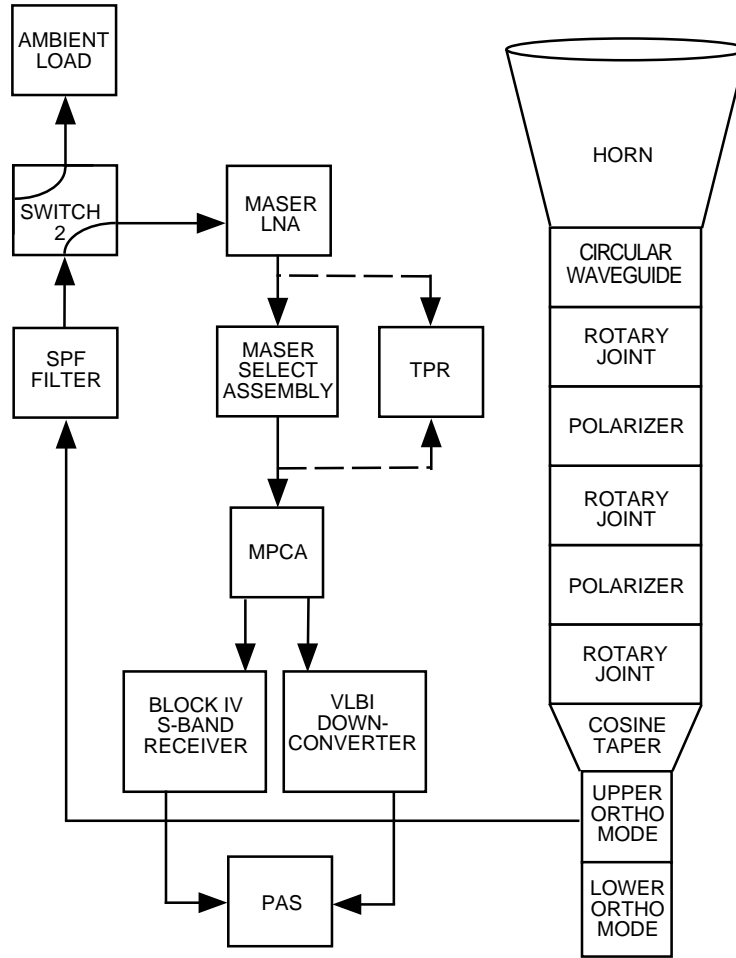


Fig. 1. The 70-m SPD diverse front-end listen-only mode for DSS 43 and DSS 63.

## II. Noise Measurement Technique

In the course of this investigation, two types of noise measurements made at different points along the front-end component string were needed to assess where the noise temperature problem was located. The first measurement is the total system noise temperature,  $T_{op}$ , while the antenna is pointed at zenith. The noise power level is measured using the 50-MHz precision attenuator assembly (PAS) or other suitable receiver. Switch 2 in Fig. 1 is switched so that the maser LNA is on the sky. Switch 2 is then switched so that the maser input is on the ambient load. The difference in power levels,  $Y$ , the Y-factor in dB, is then used to determine the  $T_{op}$ :

$$T_{op} = \frac{T_{load} + T_{rcvr}}{10^{Y/10}} \quad (1)$$

where  $T_{load}$  is the ambient load temperature, K, and  $T_{rcvr}$  is the maser input noise temperature, K, including the follow-up noise temperature (FNT) contribution. This approach is extremely accurate for  $T_{rcvr} \ll T_{load}$  and requires independent knowledge of  $T_{rcvr}$ .

The second measurement required is the FNT. This is accomplished by measuring the difference in power level in dB, the Y-factor, by using the PAS or other suitable receiver, with the maser switched to

**Table 1. Noise budget for DSS 14.<sup>a</sup>**

Component	Part number	$\Delta T$ , K	$L$ , dB	$T$ , K	$G$ , dB	$T_{in}$ , K	Noise term, K
Cosmic background	—	2.7	—	—	—	—	2.657
Atmosphere	—	1.8	—	—	—	—	1.772
Antenna spillover	—	1.44	—	—	—	—	1.417
Antenna scatter	—	2.3	—	—	—	—	2.264
Main reflector	—	0.08	—	—	—	—	0.079
Subreflector	—	0.07	—	—	—	—	0.069
Main reflector gap leakage	—	0.1	—	—	—	—	0.098
Feedhorn	9449420-1	—	0.003	293	—	—	0.199
Waveguide round	9457310-1	—	0.0015	293	—	—	0.100
Waveguide round, 15.141 in. + rotary joint 1 in.	—	—	0.0018	293	—	—	0.120
Rotary joints (2)	9457311-1	—	0.003	293	—	—	0.200
Polarizers (1)	9449405-1	—	0.0035	293	—	—	0.233
Cosine taper	9457389-1	—	0.002	293	—	—	0.133
Orthomode, upper	9457308-1	—	0.005	293	—	—	0.333
Matched coupler, 40 dB injected = 0.029 K	9457331-1	—	0.00345	293	—	—	0.230
Elbow, H-plane	9451160-2	—	0.0037	293	—	—	0.247
S-band passband filter	9430960	—	0.021	293	—	—	1.406
3-position switch	9443100-1	—	0.008	293	—	—	0.538
Elbow, E-plane	9451159-2	—	0.0037	293	—	—	0.249
Straight, 13 in.	9459426-3	—	0.003	293	—	—	0.202
35-dB coupler (loss)	SR8148D	—	0.0066	293	—	—	0.445
35-dB coupler (injected)	—	—	35	293	—	—	0.093
Maser/CCR VSWR <sup>b</sup> (not used)	—	0.00	—	—	—	—	0.000
Maser/CCR package	—	—	—	—	45	2	2.000
LP filter	—	—	0.1	293	—	—	0.000
10-dB couplers (2)	—	—	1	293	—	—	0.002
Cable loss, 1/2 in. spiraline	—	—	1.7	293	—	—	0.006
Maser select box	—	—	0.8	293	—	—	0.004
Cable	—	—	0.5	293	—	—	0.003
Loss	—	—	0	0	—	—	0.000
Avantek amplifier	AN-2200N	—	—	—	25	870	0.071
20-dB coupler	—	—	20	293	—	—	0.007
Cable	—	—	1	293	—	—	0.002
Downconverter $T_{in}$	—	—	—	—	—	8881	0.287
Total antenna system noise temperature (referred to input of maser)							15.47
Follow-up noise contribution $T_f$							0.382

<sup>a</sup> SPD feedcone, low-noise path, 2295 MHz, 90-deg elevation angle, and clear weather.

<sup>b</sup> Closed-cycle refrigerator (CCR) voltage standing-wave ratio (VSWR).

**Table 2. Noise budget for DSS 43 and DSS 63.<sup>a</sup>**

Component	Part number	$\Delta T$ , K	$L$ , dB	$T$ , K	$G$ , dB	$T_{in}$ , K	Noise term, K
Cosmic background	—	2.7	—	—	—	—	2.656
Atmosphere	—	1.9	—	—	—	—	1.869
Antenna spillover	—	1.44	—	—	—	—	1.416
Antenna scatter	—	2.3	—	—	—	—	2.262
Main reflector	—	0.08	—	—	—	—	0.079
Subreflector	—	0.07	—	—	—	—	0.069
Main reflector gap leakage	—	0.1	—	—	—	—	0.098
Feedhorn	9449420-1	—	0.003	293	—	—	0.199
Waveguide round	9457310-1	—	0.0015	293	—	—	0.100
Rotary joints (3)	9457311-1	—	0.0045	293	—	—	0.299
Polarizers (2)	9449405-1	—	0.007	293	—	—	0.466
Cosine taper	9457389-1	—	0.002	293	—	—	0.133
Orthomode, upper	9457308-1	—	0.005	293	—	—	0.333
Matching section, upper	9457331-1	—	0.003	293	—	—	0.200
Elbow, H-plane	9451160-2	—	0.0037	293	—	—	0.247
S-band passband filter	9430960	—	0.021	293	—	—	1.406
3-position switch	9443100-1	—	0.008	293	—	—	0.538
Elbow, E-plane	9451159-2	—	0.0037	293	—	—	0.249
Straight, 13 in.	9459426-3	—	0.003	293	—	—	0.202
35-dB coupler (loss)	SR8148D	—	0.0066	293	—	—	0.445
35-dB coupler (injected)	—	—	35	293	—	—	0.093
Maser/CCR <sup>b</sup> package	—	—	—	—	45	2	2.000
LP filter	—	—	0.1	293	—	—	0.000
10-dB couplers (2)	—	—	1	293	—	—	0.002
Cable loss, 1/2 in. spiraline	—	—	1.7	293	—	—	0.006
Maser select box	—	—	0.8	293	—	—	0.004
Cable	—	—	0.5	293	—	—	0.003
Avantek amplifier	AN-2200N	—	—	—	25	870	0.071
20-dB coupler	—	—	20	293	—	—	0.007
Cable	—	—	1	293	—	—	0.002
Downconverter $T_{in}$	—	—	—	—	—	8881	0.287
Total antenna system noise temperature (referred to input of maser)							15.74
Follow-up noise contribution $T_f$							0.382

<sup>a</sup> SPD feedcone, low-noise path, 2295 MHz, 90-deg elevation angle, and clear weather.

<sup>b</sup> Closed-cycle refrigerator.

the ambient load while switching the maser pump source on and off. The Y-factor,  $Y$ , is then used to determine the FNT:

$$FNT = \frac{T_{load}}{10^{Y/10}} \quad (2)$$

where  $T_{load}$  is the ambient load temperature, K, and the difference in power level between the maser pump on and off is  $Y$ , dB.

### III. Preliminary Investigation and Baseline Data

A noise budget was prepared for the DSS-14, DSS-43, and DSS-63 SPD systems in the listen-only mode. These noise budgets used our best estimates of microwave performance for each component in the system. Some measured data were available; other figures are theoretical. Measurements made at the stations were compared with these noise budget predictions. While the DSS-14 SPD system noise temperature agreed closely with its noise budget, those at DSS 43 and DSS 63 did not agree with predicted performance. Further FNT measurements isolated the problem at DSS 43 and DSS 63 to that part of the SPD system following the maser. This was determined after comparing the over-1-K FNT measured at both stations to the 0.4-K predicted noise. Since DSS 14 was the only station that closely agreed with predictions, and since it was the most readily available SPD system, it was carefully evaluated and used as a baseline against which to compare the other two stations.

A  $T_{op}$  measurement made at DSS 14 using the PAS yielded the data shown in row 1 of Table 3. A similar  $T_{op}$  measurement was made at the immediate output of the maser using the JPL total power radiometer (TPR); this yielded the data in row 2. The  $T_{op}$  measured at the input to the multipoint coupler assembly (MPCA) is shown in row 3. An FNT measurement made using the PAS gave the data in row 4, while an FNT measurement made using the JPL TPR is shown in row 5. Next, the Block IV receivers' noise performances were checked using a Hewlett Packard (HP) 8970B noise figure meter. The resulting noise figure (NF) and gain information obtained at 2295 MHz is displayed in row 6 for receiver 1 and row 7 for receiver 2.

The high noise figures and the difference in noise figures, 21.4 dB for receiver 1 and 17.3 dB for receiver 2, of the Block IV receivers were noted. This poor performance results in the  $T_{op}$  being more than 0.5-K above what good engineering practice should provide. A further explanation of the problem and a proposed solution appear in the recommendations section.

**Table 3. Measurement data for DSS 14.**

Data no., type	$Y$ , dB	Load, deg C	$T_{rcvr}$ , K	$T_{op}$ , K	FNT, K	NF, dB	Gain, dB
1, PAS	12.88	18	2.5	15.1	—	—	—
2, TPR	13.05	18	2.5	14.5	—	—	—
3, MPCA	13.05	18	2.5	14.5	—	—	—
4, PAS	25	18	—	—	0.92	—	—
5, TPR	35	18	—	—	0.04	—	—
6, Receiver 1	—	—	—	—	—	21.4	33
7, Receiver 2	—	—	—	—	—	17.3	33

## IV. DSS-43 Measurements

Measurements made at DSS 43 at the start of this investigation gave system noise temperature values of 17.2 K. Measurements made later on in the course of the investigation by station personnel at DSS 43 using the 50-MHz PAS resulted in the data in rows 1 and 3 of Table 4. These data were reduced by station personnel and, therefore, the raw data are unavailable. Measurements made at DSS 43 using the JPL TPR yielded the data in rows 2 and 4.

Station personnel explained the difference in measurements before and after evaluation activities as follows: At DSS 43, there never was a problem with the actual system noise temperature, and the precision power monitor method of measurement was reporting the correct result. The station chose to publish a determination of the system noise temperature based on a Y-factor detector result. This result was in error because of a nonstandard configuration of the Y-factor detector assembly. The station corrected this and confirmed that results from the three different methods<sup>1</sup> of measuring system noise temperature at the station agreed within 0.5 K.

**Table 4. Measurement data for DSS 43.**

Data no., type	Y, dB	Load, deg C	$T_{rcvr}$ , K	$T_{op}$ , K	FNT, K	NF, dB	Gain, dB
1, PAS	—	—	—	14.7	—	—	—
2, TPR	13.06	18.8	2.5	14.7	—	—	—
3, PAS	—	—	—	—	0.4	N/A	N/A
4, TPR	39.23	19	—	—	0.039	N/A	N/A

## V. DSS-63 Measurements

The system operating noise temperature,  $T_{op}$ , of the SPD system at DSS 63 was measured using three methods: Row 1 of Table 5 shows the measurement result using the 50-MHz PAS; row 2 shows the results using the JPL TPR at the output of the maser LNA; and row 3 shows the results using the JPL TPR at the input to the multiport coupler assembly. An FNT measurement made using the PAS gave the data in row 4, and an FNT measurement made using the JPL TPR is shown in row 5. The input noise figure of the Block IV receivers was measured using an HP 8970B noise figure meter, and the resulting noise figure and gain information obtained at 2295 MHz is displayed in row 6 for receiver 1 and row 7 for receiver 2. The VLBI downconverter input noise figure and gain for the RCP and LCP channels were measured using an automated test setup developed at JPL. These data are shown in Fig. 2, which compares the noise figures of the two channels, and Fig. 3, which compares the gains.

Included in earlier measurements were data taken of waveguide (WG) components on the ground using the S-band test horn, the TPR, and a Block IV S-band maser that was brought from JPL. These tests were inconclusive due to the interaction of the WG components; that is, the WG components must be tested as a system and not independently in order to obtain accurate results.

Plotting system noise temperature and ambient load temperature as a function of time (Fig. 4) revealed that the highest noise temperatures were occurring at the warmest load temperatures (i.e., the warmest time of the day). This was determined to be due to inadequate air conditioning in the cone, which was causing elevated physical temperatures of the WG components. The air conditioning was improved by station personnel to bring the SPD cone physical temperature down so that it more closely matched DSS 14 and DSS 43; this improved the stability of the system noise temperature over time.

<sup>1</sup> The third method uses the open-loop VLBI/radio science downconverter output and a quality spectrum analyzer for the Y-factor measurement.

**Table 5. Measurement data for DSS 63.**

Data no., type	Y, dB	Load, deg C	$T_{rcvr}$ , K	$T_{op}$ , K	FNT, K	NF, dB	Gain, dB
1, PAS	12.54	24	4.5	16.8	—	—	—
2, TPR	12.8	27.5	4.5	16.0	—	—	—
3, MPCA	12.5	27	4.5	17.1	—	—	—
4, PAS	23.8	25.5	—	—	1.25	—	—
5, TPR	39	27	—	—	0.04	—	—
6, Receiver 1	—	—	—	—	—	15.7	27
7, Receiver 2	—	—	—	—	—	15.9	30

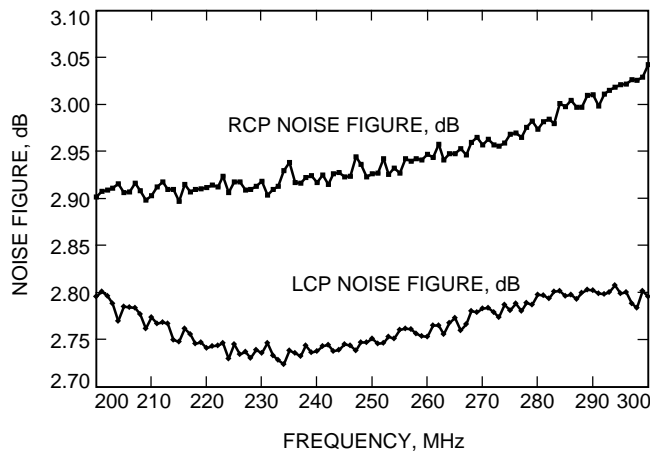


**Fig. 2. Comparison of the noise figures for the RCP and LCP channels of the VLBI downconverter at DSS 63.**

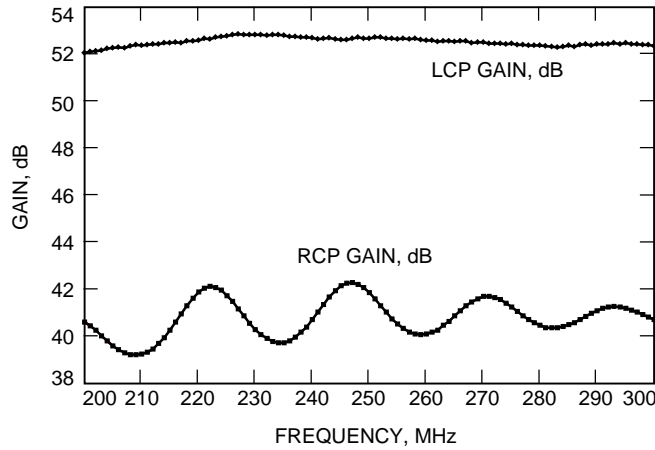


**Fig. 3. Comparison of the gain for the RCP and LCP channels of the VLBI downconverter at DSS 63.**

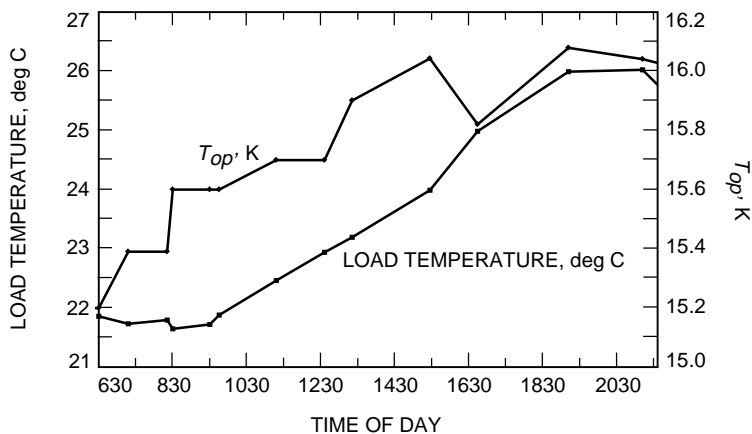


Fig. 4. Comparison of  $T_{op}$  and load temperature versus the time of day.

## VI. Conclusions

The result of the evaluation was an overall improvement of the S-band polarization diverse systems at all stations except DSS 14. DSS 14 showed a measurable increase in system noise temperature performance; this is most likely due to an elevated noise temperature in the S-band Block IV receivers at the station. Pre-evaluation results showed a  $T_{op}$  of 14.7 K, 17.2 K, and 17.6 K at DSS 14, DSS 43, and DSS 63, respectively. Postevaluation results showed a  $T_{op}$  of 15.15 K, 14.7 K, and 15.5 K at DSS 14, DSS 43, and DSS 63, respectively.

This task was successful in achieving its goals. The data taken and the equipment and procedures developed will assist in future investigations of station system noise temperatures.

## VII. Recommendations

It is recommended that tolerances be established for the 70-m SPD system  $T_{op}$  and FNT contributions at the stations. When an out-of-tolerance  $T_{op}$  is measured, the FNT and linearity should be checked, and troubleshooting should proceed to identify the problem. This could and should include use of the HP 8970B noise figure meter with an HP 346-type noise source for the purpose of noise figure and gain measurements of station equipment behind the LNA.

The Stelzried spreadsheet for checking Y-factor linearity should be implemented at all DSN stations. The stations should also have the capability of measuring the LNA noise temperature on the ground and at the output of the LNA in the cone, using the same system the JPL Microwave Electronics Group uses—a calibrated horn (for ground tests), absorber load, and the JPL total power radiometer.

The attenuators and strip chart recorders should be replaced with a precision power meter or spectrum analyzer capable of measuring Y-factor power ratios at 50 MHz with an accuracy of  $\pm 0.01$  dB.

The  $T_{op}$  of the 70-m SPD systems can be reduced an additional 0.3 K by reducing the follow-up noise temperature contribution by a factor of 10, from 0.4 to  $< 0.04$  K. This can be achieved by replacing the existing S-band follow-up amplifier with a state-of-the-art amplifier, installing this postamplifier in front of any losses between the LNA and the downconverter, and replacing the downconverters at the stations with state-of-the-art downconverters having noise figures of 5 dB or less.



The RCP channel of the VLBI downconverter at DSS 63 should be investigated. It has 14-dB less gain than the LCP channel. The fact that the RCP channel has a very similar noise figure when compared with the LCP channel indicates that this problem is in the output of the downconverter.

Finally, the two S-band Block IV downconverters at DSS 14 exhibit elevated noise temperatures. This is most likely due to an elevated loss in either the preselector filter or the mixer and should be investigated and corrected.

## **Acknowledgments**

The authors would like to thank the DSN stations and their knowledgeable personnel, who are extremely familiar with the complete end-to-end systems they operate, for their assistance during the course of this work: Larry Bracamonte at DSS 14; John Murray and Allen Robinson at DSS 43; and Jose Luis Galvez, Jose Requilme, Juan Acena, and Candido Illescas at DSS-63. We would also like to thank those people at JPL who assisted with their knowledge about specific subsystems; these include Dennis Rowan, Mike Barnard, and Sam Petty. Finally, we wish to thank Charles Stelzried for use of the linearity spreadsheet.